Theory of the anisotropy of ultrafast nonlinear refraction in zinc-blende semiconductors

D. C. Hutchings

Department of Electronics and Electrical Engineering, University of Glasgow, Glasgow G12 8QQ, United Kingdom

B. S. Wherrett

Physics Department, Heriot-Watt University, Edinburgh EH14 4AS, United Kingdom

The influence of the higher-conduction-band set Γ_{15}^c on the strength, linear/circular dichroism, and anisotropy of the ultrafast nonlinear refractive index coefficient (n_2) is calculated across the transparent spectral region below the fundamental absorption edge for the zinc-blende semiconductors GaAs and InSb. The anisotropy is due entirely to the effects of the higher bands. For GaAs, at the two-photon band edge, and for linearly polarized light, n_2 is predicted to vary by 55% as the crystal orientation is altered relative to the polarization direction. Even larger variations are expected at longer wavelengths. The far lower predicted anisotropy of InSb is consistent with the approximate formula for the strength of the anisotropy coefficient in terms of the ratio of the fundamental to the higher band gap discussed previously for two-photon absorption. The influence of such n_2 anisotropy on propagation in both one-beam and two-beam configurations is discussed. The anisotropy of the optical-switching figure of merit is also evaluated. At frequencies just below the band edge the figure is found to be greatest for radiation linearly polarized parallel to the [001] crystallographic direction; just above the half-band gap and at lower frequencies [111] linear polarization or any circular polarization is favored.

I. INTRODUCTION

Semiconductor waveguide devices show great promise for integrated, compact, high-bandwidth all-optical switches, the switching mechanism being mediated by the ultrafast nonlinear refraction of the semiconductor.[1] The presence of two-photon absorption (2PA) can be detrimental to switching. One therefore selects a material that has a band gap greater than twice the radiation photon energy in order to avoid 2PA ($Al_xGa_{1-x}As$ in the cases of the optical communication wavelengths 1.3 μm and 1.55 μm[2,3]). Alternatively the material switching figure of merit, which is proportional to the ratio of the coefficients of nonlinear refraction and two-photon absorption, must exceed a given critical value.[4] It is therefore important to understand the dependence of these two parameters on the choice of material, their frequency and polarization dependence, and their dependence on the orientation of the crystal with respect to the radiation polarization. To this end, the detailed calculations of the two-photon absorption coefficient, reported in Ref. 5, are extended here to the determination of the nonlinear refraction, using the same band-structure model.

A simple, two-band model, has proved extremely useful as a first prediction for the material scaling and the frequency dependence of the nonlinear refractive index (n_2) over a wide range of crystalline solids, from narrow-gap semiconductors through to insulating materials.[6,7] Recently the zinc-blende semiconductors have been treated in more detail, employing the valence-conduction-band-

structure model in which there are four doubly degenerate, nonparabolic bands.[1] This model contains within it the linear/circular dichroism of n_2; that is, it produces different values of n_2 for linear and circular radiation polarizations.[8]

The above models have also been employed to calculate the two-photon absorption coefficient (again with success in the two-band model in fitting to experimental results across a wide range of crystals[9]) and its dichroism (in the four-band model[10,11]). In the two-photon absorption case a third model has been used, incorporating the next higher conduction bands in order to include the dominant contributions to the crystal anisotropy of the 2PA coefficient (β).[5] It is this seven-band model that is used herein to make the first detailed calculations of the anisotropy of the coefficient of nonlinear refraction.

The zinc-blende semiconductors have cubic symmetry and as such do not exhibit linear birefringence; in the linear regime they behave as isotropic materials, with a first-order optical susceptibility tensor proportional to the unit matrix. By contrast, the third-order optical susceptibility tensor, to which n_2 and β are related, contains some nonzero off-diagonal elements. As a result complicated polarization behaviors are possible in the nonlinear regime. These are manifested in two ways. First, the state of optical polarization (linear, elliptical, or circular) influences the values of n_2 and β. Second, the orientation of the polarization with respect to the crystal axes influences them. The former effect, in so far as n_2 is concerned, produces in single-beam experiments a difference in the self-phase modulation experi-

enced for linearly and circularly polarized light. For two-beam configurations there are, for example, differences in the cross-phase modulation seen by beams of identical or orthogonal polarizations.[8] These differences can occur even for isotropic media. The crystal anisotropy leads in addition to polarization rotation in both single-beam (irradiance-dependent polarization-plane self-rotation[12]) and two-beam configurations as well as to an orientation dependence of the self- and cross-phase modulations. For nonlinear refraction, both aspects above can be thought of as a nonlinear (induced) birefringence; but in the former case, the optic axis is determined solely by the radiation polarization orientation and in the latter case incorporates the crystalline axes orientation. This crystalline-orientation dependence can occur in cubic crystals but does not exist for isotropic media.

Similar polarization-state and crystal-orientation dependencies are displayed in two-photon absorption,[5] and in third-harmonic generation. The 2PA anisotropy can lead to a polarization distortion similar to the rotation produced by anisotropy in n_2. In the third-harmonic case the anisotropy is observable both as an orientation dependence of the magnitude of the generation efficiency and as a possibility of generating third-harmonic light of polarization orthogonal to the fundamental.[13]

There are few papers reporting direct observation of the variation of the magnitude of either nonlinear absorption or nonlinear refraction with crystalline orientation in zinc-blende semiconductors. In 1975, Bepko[14] demonstrated that the two-photon absorption coefficient in GaAs is anisotropic. Two years later Van der Ziel[15] used band-edge luminescence to determine accurately the anisotropy of the GaAs two-photon absorption coefficient at 1.55 μm. More recently, picosecond measurements have been used to determine the anisotropy of the two-photon absorption coefficient in GaAs at 1.06 μm[16] and in GaAs and CdTe at 0.95 μm.[17] There have been a number of reports on the crystalline-orientation dependence of nonlinear refraction in alkali metal salts and oxides (cubic symmetry).[16,18–21] However, in semiconductors the only direct measurement of the anisotropy of n_2 to date has been in wurtzite (hexagonal) structures, which exhibit anisotropy even in the first-order susceptibility (uniaxial birefringence).[22] Resonant nonlinearities in semiconductors have been shown to exhibit orientational effects.[23,24] These phenomena can only be observed on picosecond time scales as momentum and spin relaxation causes the initial anisotropic (in k space) carrier excitation to develop into a thermalized, isotropic distribution. However, there is currently a lack of direct measurements of the anisotropy of nonresonant nonlinear refraction in zinc-blende (cubic) semiconductors.

The change of the optical polarization state due to third-order optical nonlinearities has been referred to as self-induced optical activity or nonlinear optical activity.[12] This phenomenon has been observed in GaAs at wavelengths for which it can largely be attributed to the anisotropy of the two-photon absorption coefficient.[25–27] A simple explanation of this phenomenon is that the difference between nonlinear absorption coefficients for different crystalline directions results

in a net rotation of the polarization vector towards the direction for which the absorption coefficient is a minimum. The change in the optical polarization state has also been utilized in recent two-beam Kerr ellipsometry measurements on GaAs, CdTe, and ZnSe.[28] Here measurements with and without a quarter-wave plate enabled the nonlinear absorption and refraction effects to be quantified separately. An excite-probe configuration in which the two-beams were linear polarized at a relative angle of 45° was employed in this experiment. Although there is an isotropic contribution to the change in polarization,[29] the anisotropic contribution was isolated by repeating the measurement for different crystalline orientations.

Following a unified description of the macroscopic polarizations that produce the phenomena originating from the anisotropy of the nonlinear susceptibility, both for single-beam and two-beam configurations (Sec. II), the microscopic theory for the real part of the third-order susceptibility and the results of calculations for GaAs and InSb are presented in Sec. III. These results are discussed in the context of available experimental evidence and with regard to the optical-switching figure of merit in Sec. IV.

II. MACROSCOPIC THEORY

The general form of the contribution to the third-order polarization in the frequency domain is given by[30]

$$
\begin{aligned}
\mathcal{P}_a^{(3)}(\omega) = \epsilon_0 &\int_{-\infty}^{\infty} d\omega_1 \int_{-\infty}^{\infty} d\omega_2 \int_{-\infty}^{\infty} d\omega_3 \\
&\times \sum_{ijkl} a_i^* b_j c_k d_l \chi_{ijkl}^{(3)} (\omega_1, \omega_2, \omega_3) \\
&\times \mathcal{E}_b(\omega_1)\mathcal{E}_c(\omega_2)\mathcal{E}_d(\omega_3)\delta(\omega - \omega_1 - \omega_2 - \omega_3) ,
\end{aligned}
\tag{1}
$$

where $a_i = \hat{\mathbf{a}} \cdot \hat{\mathbf{i}}$, $b_j = \hat{\mathbf{b}} \cdot \hat{\mathbf{j}}$, $c_k = \hat{\mathbf{c}} \cdot \hat{\mathbf{k}}$, and $d_l = \hat{\mathbf{d}} \cdot \hat{\mathbf{l}}$ are the direction cosines for the projections of $\mathcal{P}_a^{(3)}$, $\mathcal{E}_b$, $\mathcal{E}_c$, and $\mathcal{E}_d$ onto the directions $\hat{\mathbf{i}}$, $\hat{\mathbf{j}}$, $\hat{\mathbf{k}}$, and $\hat{\mathbf{l}}$, respectively. The unit vectors and direction cosines are allowed to be complex, in general, to allow, for example, for circular polarizations.

A. Single-beam configuration

In the case of a single monochromatic wave of frequency ω_0,

$$
\mathcal{E}(\omega) = \frac{1}{2}[\hat{\mathbf{e}}E_0\delta(\omega - \omega_0) + \hat{\mathbf{e}}^*E_0^*\delta(\omega + \omega_0)] ,
\tag{2}
$$

the contribution to the third-order polarization in a cubic crystal at frequency ω_0 is

$$
\mathcal{P}_a^{(3)}(\omega)\Big|_{\omega_0} = \frac{3}{8}\epsilon_0\chi_{\text{eff}}(a; e^*, e, e)|E_0|^2 E_0\delta(\omega - \omega_0) .
\tag{3}
$$

In Eq. (3),

$$\mathrm{Re}\chi_{\mathrm{eff}}(a; e^*, e, e) = (\hat{\mathbf{a}}^* \cdot \hat{\mathbf{e}}^*)(\hat{\mathbf{e}} \cdot \hat{\mathbf{e}})\chi'_{xxyy}$$
$$+ 2(\hat{\mathbf{a}}^* \cdot \hat{\mathbf{e}})\chi'_{xyxy}$$
$$+ \sigma' \chi'_{xxxx} \sum_i a_i^* e_i |e_i|^2 \,,$$

$$\mathrm{Im}\chi_{\mathrm{eff}}(a; e^*, e, e) = (\hat{\mathbf{a}}^* \cdot \hat{\mathbf{e}}^*)(\hat{\mathbf{e}} \cdot \hat{\mathbf{e}})\chi''_{xxyy}$$
$$+ 2(\hat{\mathbf{a}}^* \cdot \hat{\mathbf{e}})\chi''_{xyxy}$$
$$+ \sigma'' \chi''_{xxxx} \sum_i a_i^* e_i |e_i|^2 \,, \qquad (4)$$

where we have used, for example, χ'_{xxyy} and χ''_{xxyy} as a shorthand form for the real and imaginary parts of $\chi^{(3)}_{xxyy}(-\omega_0, \omega_0, \omega_0)$, respectively. With this notation, the anisotropy parameters σ' and σ'' are defined by the ratios,

$$\sigma' = \frac{\chi'_{xxxx} - \chi'_{xxyy} - 2\chi'_{xyxy}}{\chi'_{xxxx}} \,, \qquad (5)$$

$$\sigma'' = \frac{\chi''_{xxxx} - \chi''_{xxyy} - 2\chi''_{xyxy}}{\chi''_{xxxx}} \,. \qquad (6)$$

The nonlinear absorptive anisotropy σ'' arising from two-photon absorption has been considered previously, in Ref. 5.

There are two aspects of Eq. (3) that require consideration. First, there is a contribution to the nonlinear polarization with the same polarization state as the input wave, $\hat{\mathbf{a}} = \hat{\mathbf{e}}$, for which the effective nonlinearity is

$$\mathrm{Re}\chi_{\mathrm{eff}}(e; e^*, e, e) = |\hat{\mathbf{e}} \cdot \hat{\mathbf{e}}|^2 \chi'_{xxyy} + 2\chi'_{xyxy}$$
$$+ \sigma' \chi'_{xxxx} \sum_i |e_i|^4 \,, \qquad (7)$$

with the equivalent form for the imaginary part.

Second, there is, in general, an additional nonlinear induced polarization, which changes the polarization state of the propagating wave. It is appropriate to examine the contribution to the nonlinear polarization with a polarization vector orthogonal to the input, $\hat{\mathbf{a}} = \hat{\mathbf{q}}$. For linear polarization, $\hat{\mathbf{q}} \cdot \hat{\mathbf{e}} = 0$ and $\hat{\mathbf{q}}^* \cdot \hat{\mathbf{e}} = 0$, while for circular polarization $\hat{\mathbf{q}} \cdot \hat{\mathbf{e}} = 1$, $\hat{\mathbf{q}}^* \cdot \hat{\mathbf{e}} = \hat{\mathbf{e}} \cdot \hat{\mathbf{e}} = 0$. In either case the effective nonlinear contribution is

$$\mathrm{Re}\chi_{\mathrm{eff}}(q; e^*, e, e) = \sigma' \chi'_{xxxx} \sum_i q_i^* e_i |e_i|^2 \,. \qquad (8)$$

This result exhibits the fact that the third-order susceptibility can only cause the polarization state to change through the anisotropy of the crystal.

It is of interest to consider those polarization orientations for which this orthogonal contribution is zero and the polarization state is preserved even in the presence of anisotropy. Consider a propagation direction defined in spherical coordinates with respect to the crystal axes by the unit vector, $\hat{\mathbf{k}} = (\sin\theta\cos\phi, \sin\theta\sin\phi, \cos\theta)$. Construct a unit vector perpendicular to this and lying in the xy plane, $\hat{\mathbf{e}}_1 = (\sin\phi, -\cos\phi, 0)$ and a third unit vector perpendicular to both $\hat{\mathbf{k}}$ and $\hat{\mathbf{e}}_1$, $\hat{\mathbf{e}}_2 = \hat{\mathbf{k}} \times \hat{\mathbf{e}}_1 = (\cos\theta\cos\phi, \cos\theta\sin\phi, -\sin\theta)$. The general form of the unit polarization vector in the case of linearly polarized light for this propagation direction is given by the linear combination, $\hat{\mathbf{e}} = \hat{\mathbf{e}}_1\cos\psi + \hat{\mathbf{e}}_2\sin\psi$, where ψ defines the polarization vector orientation with respect to the xy plane. This allows the perpendicular unit vector $\hat{\mathbf{q}}$ to be written as $\hat{\mathbf{q}} = \hat{\mathbf{e}}_1\sin\psi - \hat{\mathbf{e}}_2\cos\psi$. The condition $\sum_i q_i^* e_i |e_i|^2 = 0$, for which the polarization state is preserved, then forms a transcendental equation for the polarization orientation ψ in terms of the propagation direction (θ, ϕ),

$$(\sin\phi\sin\psi - \cos\theta\cos\phi\cos\psi)(\sin\phi\cos\psi + \cos\theta\cos\phi\sin\psi)^3 + (\cos\phi\sin\psi + \cos\theta\sin\phi\cos\psi)$$
$$\times (\cos\phi\cos\psi - \cos\theta\sin\phi\sin\psi)^3 - \sin^4\theta\cos\psi\sin^3\psi = 0 \,. \qquad (9)$$

This transcendental equation provides eight roots for ψ in the range $0 \le \psi < 2\pi$, except when the propagation direction is parallel to one of the eight directions equivalent to [111] when Eq. (9) is satisfied for any value of ψ. The linear polarization orientations, which solve Eq. (9) and hence preserve the polarization state, are shown in Table I for the three propagation directions [100], [110], and [111].

A similar analysis can be performed in the case of circularly polarized light where $\hat{\mathbf{e}} = (\hat{\mathbf{e}}_1 + i\hat{\mathbf{e}}_2)/\sqrt{2}$ and $\hat{\mathbf{q}} = $

$(\hat{\mathbf{e}}_1 - i\hat{\mathbf{e}}_2)/\sqrt{2}$. In this case the condition $\sum_i q_i^* e_i |e_i|^2 = 0$ represents a constraint on the propagation direction (θ, ϕ). It can be shown that this condition is only satisfied if the propagation direction is parallel either to one of the six directions equivalent to [100] or to one of the eight directions equivalent to [111].

In the cases where the polarization state of the input wave is preserved, one can describe the effect of the real part of χ_{eff} through a nonlinear refractive index $n_2(\omega)$, defined through the first-order change in the refractive

TABLE I. Single-beam configurations under which the linear polarization is preserved.

$\hat{\mathbf{k}} \parallel$	$\hat{\mathbf{e}} \parallel$							
[100]	[010]	[011]	[001]	[0$\bar{1}$1]	[0$\bar{1}$0]	[0$\bar{1}$$\bar{1}$]	[00$\bar{1}$]	[01$\bar{1}$]
[110]	[1$\bar{1}$0]	[1$\bar{1}$1]	[001]	[$\bar{1}$11]	[$\bar{1}$10]	[$\bar{1}$1$\bar{1}$]	[00$\bar{1}$]	[1$\bar{1}$$\bar{1}$]
[111]	any polarization orientation							

index n with irradiance I, $(n = n_0 + n_2 I)$,

$$n_2(\omega) = \frac{3}{4\epsilon_0 c n_0^2} \mathrm{Re}\chi_{\mathrm{eff}}(e; e^*, e, e) \ ,$$

$$= \frac{3}{4\epsilon_0 c n_0^2} \left[|\hat{\mathbf{e}} \cdot \hat{\mathbf{e}}|^2 \, \chi'_{xxyy} + 2\chi'_{xyxy} \right.$$

$$\left. + \sigma' \chi'_{xxxx} \sum_i |e_i|^4 \right] \ . \qquad (10)$$

It is convenient to translate the three independent third-order susceptibility tensor elements into three parameters that describe the strength, anisotropy, and dichroism of the nonlinear refraction in the same manner as has been done for two-photon absorption.[5] For the strength it is appropriate to use the n_2 coefficient for light linearly polarized parallel to a principal crystal axis. For the anisotropy, the refractive anisotropy parameter σ' defined in Eq. (5) is used. For the third practical parameter, an incremental dichroism (δ') has previously been introduced in Ref. 8; this relates the different n_2 values for linear and circular polarizations. The same parameter, modified for anisotropic systems, will be employed here. These parameters can be determined by three measurements of n_2 (two for linear and one for circular polarization) for light propagating along a principal axis,

$$n_2^L[001] = \frac{3}{4\epsilon_0 c n_0^2} \mathrm{Re}\chi'_{xxxx} \ , \qquad (11)$$

$$\sigma' = \frac{\chi'_{xxxx} - \chi'_{xxyy} - 2\chi'_{xyxy}}{\chi'_{xxxx}}$$

$$= 2 \frac{n_2^L[001] - n_2^L[011]}{n_2^L[001]} \ , \qquad (12)$$

$$\delta' = \frac{\chi'_{xxxx} + \chi'_{xxyy} - 2\chi'_{xyxy}}{2\chi'_{xxxx}}$$

$$= \frac{n_2^L[001] - n_2^C(\mathbf{k} \parallel [100])}{n_2^L[001]} \ . \qquad (13)$$

Using these parameters, Eq. (10) can be rewritten, for linear and circular polarizations, respectively, in the form

$$n_2^L(\theta_p, \phi_p) = n_2^L[001] \left[1 - \frac{\sigma'}{2} (\sin^2 2\theta_p \right.$$

$$\left. + \sin^4 \theta_p \sin^2 2\phi_p) \right] \ ,$$

$$n_2^C(\theta, \phi) = n_2^L[001] \left[1 - \delta' - \frac{\sigma'}{8} (\sin^2 2\theta \right.$$

$$\left. + \sin^4 \theta \sin^2 2\phi) \right] \ , \qquad (14)$$

where (θ_p, ϕ_p) refers to the optical polarization orientation with respect to the crystal axes and (θ, ϕ) refers to the propagation direction.

For the case where the polarization state can change,

Eqs. (3) and (8) allow the determination of the evolution of the generated orthogonally polarized wave. If a low conversion efficiency is assumed (such that the excite irradiance can be treated as constant) and if there is initially no orthogonal component, the real part of the third-order susceptibility generates in a crystal of length L an irradiance,

$$I_q = \frac{\omega^2 L^2}{c^2} \left(\sigma' n_2^L[001] \sum_i q_i^* e_i |e_i|^2 \right)^2 I_e^3 \ . \qquad (15)$$

The phase of this generated orthogonal component is $\pi/2$ different from the input, resulting in a net elliptical polarized output from a linearly polarized input. In the case of the imaginary part of the third-order susceptibility, a similar result is obtained except the generated orthogonal component is in phase with respect to the input and hence a net polarization rotation results from a linearly polarized input.

B. Two-beam configuration

In addition to the self-phase modulation considered above, it is of interest to consider the cross-phase modulation between two waves. Consider an input consisting of an excite wave and probe wave, where the amplitude of the probe is much smaller than that of the excite $E_p \ll E_e$,

$$\mathcal{E}(\omega) = \frac{1}{2} \left[\hat{\mathbf{e}} E_e \delta(\omega - \omega_e) + \hat{\mathbf{e}}^* E_e^* \delta(\omega + \omega_e) \right]$$

$$+ \frac{1}{2} \left[\hat{\mathbf{p}} E_p \delta(\omega - \omega_p) + \hat{\mathbf{p}}^* E_p^* \delta(\omega + \omega_p) \right] \ . \qquad (16)$$

For cross-phase modulation from the excite wave onto the probe, the nonlinear polarization contributions are

$$\mathcal{P}_a^{(3)}(\omega)\Big|_{\omega_p} = \frac{3}{4}\epsilon_0 |E_e|^2 E_p \delta(\omega - \omega_p)$$

$$\times \sum_{ijkl} a_i^* e_j^* e_k p_l \chi_{ijkl}^{(3)} (-\omega_e, \omega_e, \omega_p) \ ,$$

$$\qquad (17)$$

$$\mathcal{P}_a^{(3)}(\omega)\Big|_{2\omega_e - \omega_p} = \frac{3}{8}\epsilon_0 E_p^* E_e^2 \delta(\omega - 2\omega_e + \omega_p)$$

$$\times \sum_{ijkl} a_i^* p_j^* e_k e_l \chi_{ijkl}^{(3)} (-\omega_p, \omega_e, \omega_e) \ .$$

$$\qquad (18)$$

The polarization described by Eq. (17) is a source for radiation at the probe frequency and propagating in the probe direction. (It is automatically phase matched with the probe wave.) In contrast, Eq. (18) describes the generation of a field at frequency $(2\omega_e - \omega_p)$ and propagating in the direction $(2\mathbf{k}_e - \mathbf{k}_p)$. We have in mind the situation in which the frequencies are degenerate but the two beams are distinguished either by propagation direction $(\mathbf{k}_e \neq \mathbf{k}_p)$ or by polarization direction $(\hat{\mathbf{p}} \neq \hat{\mathbf{e}})$. The influence on the probe beam will be small, due to the lack of phase matching, if the sample length is large

compared to the coherence length, $L_c = \pi/(2|\mathbf{k}_p - \mathbf{k}_e|)$. The contribution from Eq. (18) can then be neglected for noncollinear propagation or for collinear propagation of orthogonally polarized modes in a waveguide configuration where the different propagation constants lead to a phase mis-match. The remaining case, in which differently polarized but collinear beams are input, can be treated as a single-beam experiment (with amplitude and polarization given by the resultants of those for the two beams) if the two beams are coherent with each other. In the case of incoherent beams, the time average of Eq. (18) is zero and hence can also be neglected. We shall therefore discuss here only the effect of the polarization contribution of Eq. (17). Keeping just those tensor elements that contribute for zinc-blende symmetry, results in a nonlinear polarization contribution

$$\mathcal{P}_a^{(3)}(\omega)\Big|_{\omega_p} = \frac{3}{4}\epsilon_0\chi_{\text{eff}}(a; e^*, e, p)|E_e|^2 E_p \delta(\omega - \omega_p) , \quad (19)$$

where

$$
\begin{aligned}
\text{Re}\chi_{\text{eff}}(a; e^*, e, p) = &(\hat{\mathbf{a}}^* \cdot \hat{\mathbf{e}}^*)(\hat{\mathbf{p}} \cdot \hat{\mathbf{e}}) \chi'_{xxyy} \\
&+ (\hat{\mathbf{a}}^* \cdot \hat{\mathbf{e}})(\hat{\mathbf{p}} \cdot \hat{\mathbf{e}}^*) \chi'_{xyxy} \\
&+ (\hat{\mathbf{a}}^* \cdot \hat{\mathbf{p}}) \chi'_{xyyx} \\
&+ \sigma'\chi'_{xxxx} \sum_i a_i^* p_i |e_i|^2 ,
\end{aligned}
\quad (20)
$$

with an equivalent expression for $\text{Im}\chi_{\text{eff}}(a; e^*, e, p)$, which could correspond to, for example, nondegenerate two-photon absorption.[10] In the nondegenerate case, the frequency ordering referred to by the shorthand form is $\chi'_{xxyy} = \text{Re}\chi^{(3)}_{xxyy}(-\omega_e, \omega_e, \omega_p)$. Note that an additional factor of 2 is obtained for cross-phase modulation by comparison to the equivalent expression for self-phase modulation in Eq. (3). It is appropriate to consider the contributions with polarization vectors equal to and orthogonal to the probe polarization. In the former case $\hat{\mathbf{a}} = \hat{\mathbf{p}}$ and

$$
\begin{aligned}
\text{Re}\chi_{\text{eff}}(p; e^*, e, p) = &|\hat{\mathbf{p}} \cdot \hat{\mathbf{e}}|^2 \chi'_{xxyy} + |\hat{\mathbf{p}} \cdot \hat{\mathbf{e}}^*|^2 \chi'_{xyxy} \\
&+ \chi'_{xyyx} + \sigma'\chi'_{xxxx} \sum_i |p_i|^2 |e_i|^2 .
\end{aligned}
\quad (21)
$$

The contribution to the nonlinear polarization with polarization vector $\hat{\mathbf{q}}$ orthogonal to the probe polarization vector is given by

$$
\begin{aligned}
\text{Re}\chi_{\text{eff}}(q; e^*, e, p) = &(\hat{\mathbf{q}}^* \cdot \hat{\mathbf{e}}^*)(\hat{\mathbf{p}} \cdot \hat{\mathbf{e}}) \chi'_{xxyy} \\
&+ (\hat{\mathbf{q}}^* \cdot \hat{\mathbf{e}})(\hat{\mathbf{p}} \cdot \hat{\mathbf{e}}^*) \chi'_{xyxy} \\
&+ \sigma'\chi'_{xxxx} \sum_i q_i^* p_i |e_i|^2 .
\end{aligned}
\quad (22)
$$

Two contributions to this orthogonal polarization can be identified in the excite-probe case. The first two terms in Eq. (22) depend only on the relative orientation of excite and probe polarizations. In the case of linear polarizations, this contribution is zero if the excite and probe polarization vectors are either parallel or perpendicular. In fact this contribution can be thought of as an induced birefringence for the probe beam with the excite polar-

ization vector defining the optic axis.[28,29] If the probe polarization is such that it initially has both ordinary ray and extraordinary ray components, the vector sum will change on propagation. Specifically, from a linear polarized input, $\text{Re}\chi_{\text{eff}}(q; e^*, e, p)$ will induce a degree of ellipticity into the polarization and $\text{Im}\chi_{\text{eff}}(q; e^*, e, p)$ will cause a net rotation of the polarization vector. The final term in Eq. (22) is a crystalline-orientational dependence term proportional to the anisotropy. This orientation dependent term can be isolated experimentally by comparing Kerr ellipsometry measurements for two different crystalline orientations.[28]

The contribution given by Eq. (22) can be eliminated by a suitable choice of experimental geometry, just as the single-beam polarization rotation term could be eliminated. Hence, under a number of specific configurations there will be no change in the state of the polarization vector. Example configurations are (a) for linear polarizations in the parallel polarized case $\hat{\mathbf{p}} \parallel \hat{\mathbf{e}} \parallel [001]$, [011], or [111], or in the perpendicular polarized case for the $(\hat{\mathbf{p}}, \hat{\mathbf{e}})$ pairs parallel to ([001],[110]), ([110],[1$\bar{1}$0]), or ([111],[1$\bar{1}$0]) and (b) for circular polarizations propagating along a principal axis with either circular polarization for the probe compared to the excite beam. In these cases, the real part of the third-order nonlinearity gives rise only to a nonlinear phase shift in the probe beam that is proportional to the irradiance of the excite beam,

$$
\begin{aligned}
\Delta n(\omega_p) &= \frac{3}{2\epsilon_0 c n_0^2} \text{Re}\chi_{\text{eff}}(p; e^*, e, p) I_e , \\
&= \frac{3}{2\epsilon_0 c n_0^2} \Big[|\hat{\mathbf{p}} \cdot \hat{\mathbf{e}}|^2 \chi'_{xxyy} + |\hat{\mathbf{p}} \cdot \hat{\mathbf{e}}^*|^2 \chi'_{xyxy} \\
&\quad + \chi'_{xyyx} + \sigma'\chi'_{xxxx} \sum_i |p_i|^2 |e_i|^2 \Big] I_e .
\end{aligned}
\quad (23)
$$

There are four special cases of this cross-phase modulation where both beams have the same frequency: probe and excite polarization vectors parallel and orthogonal in the cases of linear polarizations and circular polarizations. For these cases, the ratio $\chi'_{\text{eff}}/\chi'_{xxxx} = \Delta n_p/(2n_2^L[001]I_e)$ is related to the parameters σ' and δ' as shown in Table II. Note that the use of two-beam experiments provides an alternative means of measuring the practical parameters and hence the nonlinear tensor elements. In particular in waveguide geometries where only linearly polarized guided modes are supported, the incremental dichroism parameter can be determined by measuring the cross-phase modulation between TE and TM modes.[31]

TABLE II. $\chi'_{\text{eff}}/\chi'_{xxxx}$ for four degenerate-frequency, noncollinear excite-probe configurations.

Linear	$\hat{\mathbf{p}} \parallel \hat{\mathbf{e}}$	$1 + \sigma'\left(\sum_i |e_i|^4 - 1\right)$
	$\hat{\mathbf{p}} \perp \hat{\mathbf{e}}$	$\frac{1}{2}(1 - \delta') + \sigma'\left(\sum_i |p_i|^2|e_i|^2 - \frac{1}{4}\right)$
Circular	$\hat{\mathbf{p}} = \hat{\mathbf{e}}$	$(1 - \delta') + \sigma'\left(\sum_i |e_i|^4 - \frac{1}{2}\right)$
	$\hat{\mathbf{p}} = \hat{\mathbf{e}}^*$	$\frac{1}{2}(1 + \delta') + \sigma'\left(\sum_i |e_i|^4 - \frac{3}{4}\right)$

III. MICROSCOPIC THEORY

The expressions for the third-order susceptibility tensor elements are detailed in Ref. 8, in which the four-band Kane model[32] was employed. However, this model is isotropic and hence it is insufficient to account for the anisotropy of the nonlinear refraction. The approach taken here is to include additionally the contribution from the next higher-conduction-band set Γ_{15}^c[33] as has previously been employed to determine the anisotropy of the two-photon absorption coefficient.[5] Essentially the band energies and wave functions are obtained by diagonalization of a 14×14 matrix. This is performed numerically and so automatically includes higher-order terms in k, which give rise to such effects as nonparabolicity. The sum over electronic states is performed using the Pauli-allowed approach[1,34] in order to avoid spuriously diverging terms associated with intervalence virtual transitions.

In the determination of n_2 using the Kane model[1,8] it was possible to perform the integration over the electronic wave vector k out to infinity. However, while this band-structure model gives a good approximation to the electronic states near zone center, it is inaccurate for the states in the vicinity of the Brillioun zone boundary. As a result of this inaccuracy, the calculated susceptibility tensor elements have unphysical contributions that behave as ω^{-4} and ω^{-2} and hence apparently diverge at zero frequency. As in the four-band calculations,[1] n_2 is obtained by expanding the calculated susceptibility tensor element as a Laurent series and simply subtracting these diverging terms. However, with the inclusion of the upper-conduction-band set it is found that the integral over k does not converge even for finite frequencies. The reason behind this is that while in the Kane band model the asymptotic behavior of the conduction-band energy at high k is proportional to k, with the inclusion of the higher conduction bands, the conduction-band energy asymptotes to a constant (maximum) value instead. Hence the energy denominators in the $\chi^{(3)}$ expression tend to constants at high k values and the resulting contributions to $\chi^{(3)}$ do not tend to zero. To avoid the resulting divergence, here the integration over k is taken to a large but finite value. The results shown below are calculated for $\hbar k_{\text{max}}/\sqrt{2m_0} = 0.6$ (eV)$^{1/2}$, which corresponds to approximately half the Brillouin zone boundary. It was found that by changing this cutoff value that the calculated susceptibility varied but only in the unphysical terms that diverge at zero frequency and not in the underlying contribution.

The calculated dispersion of the real part of the third-order susceptibility is shown in Fig. 1 for GaAs and InSb, based on low-temperature data.[33,35] For GaAs, the effect of the additional upper-conduction-band set is to reduce somewhat the diagonal tensor element $\text{Re}\chi_{xxxx}^{(3)}$ and to enhance the off-diagonal elements $\text{Re}\chi_{xyxy}^{(3)}$ and $\text{Re}\chi_{xxyy}^{(3)}$. As in the case of two-photon absorption,[11] the largest change occurs for the $xxyy$ tensor element. The same anisotropic effects occur for InSb, but to a very much reduced extent because the higher conduction bands are relatively well displaced with respect to the
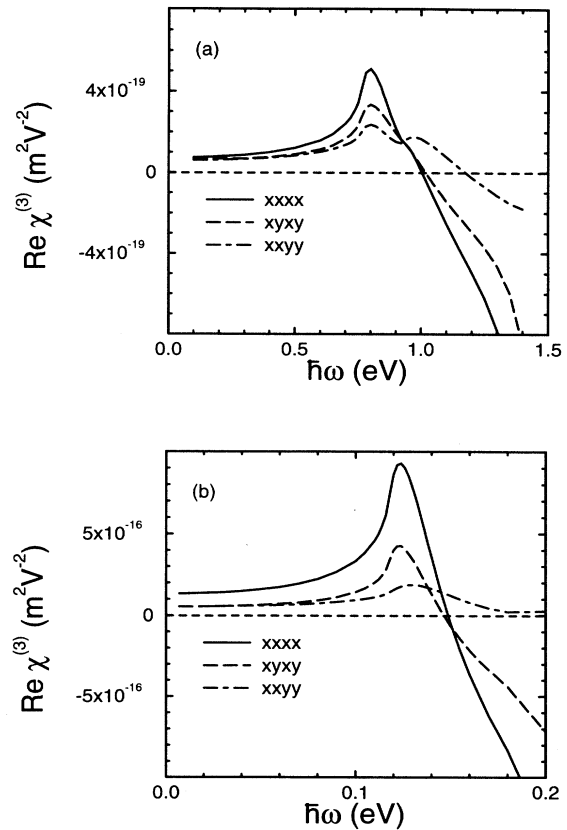

FIG. 1. Calculated dispersion of the three nonzero, independent third-order susceptibility tensor elements for (a) GaAs and (b) InSb.

valence-conduction-band set.

The calculated third-order susceptibilities are used to obtain the dispersion of the anisotropy and dichroism parameters, which are shown in Fig. 2 for GaAs and in Fig. 3 for InSb. Note that these ratios diverge at the frequency for which $\chi_{xxxx}' = 0$, but that the anisotropic contribution to the nonlinear polarization is proportional to the product $\sigma' \chi_{xxxx}'$, which remains finite. To illustrate this, the products $\sigma' \chi_{xxxx}'$ and $\delta' \chi_{xxxx}'$ are also shown. Note that for GaAs the product $\sigma' \chi_{xxxx}'$ is shown on a similar scale to χ_{xxxx}' in Fig. 1(a) but for InSb it is shown on a scale that is approximately an order of magnitude less than in Fig. 1(b). In the case of the dichroism parameter, a comparison is made with the results of the four-band model. Because the incremental dichroism is defined with respect to the index for $\hat{e} \parallel [001]$, which is the minimum value, the extreme of the difference between the two models is plotted here; the change in dichroism, brought about by introducing the higher conduction bands, is smaller for other polarization directions. To demonstrate this, the ratio $(n_2^L - n_2^C)/n_2^L$ is shown for the propagation direction $\mathbf{k} \parallel [111]$, for which there is no angular variation of n_2^L. It can be seen that for both GaAs and InSb this value is close to the four-band model incremental dichroism; an equivalent similarity was also
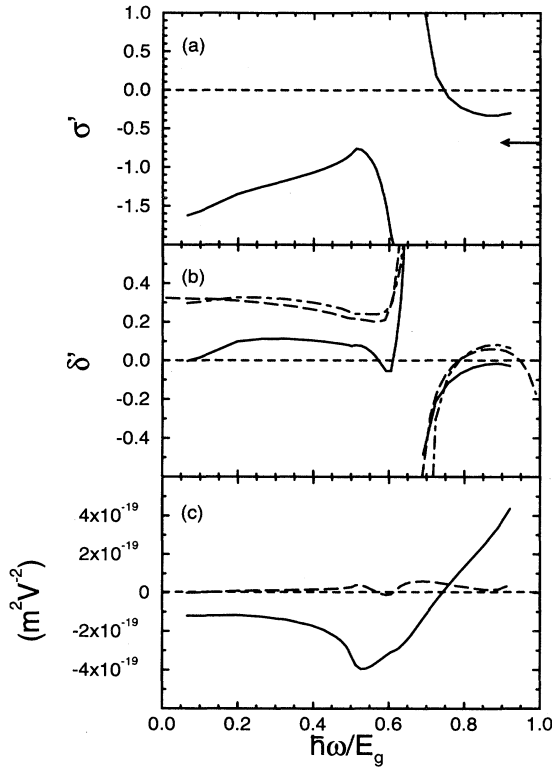
FIG. 2. Dispersion of the nonlinear refractive ratios for GaAs: (a) shows the refractive anisotropy parameter with the arrow indicating the value of the ratio $-2E_g/(E_g + E_u)$ (see text); (b) shows the refractive incremental dichroism parameter, for the seven-band model (solid), the four-band model (dashed), and the incremental dichroism for $\mathbf{k} \parallel$ [111] (chain) (see text); (c) shows the products $\sigma'\chi'_{xxxx}$ (solid) and $\delta'\chi'_{xxxx}$ (dashed), indicating that although the ratios have divergences, the contribution to the effective susceptibility remains finite.
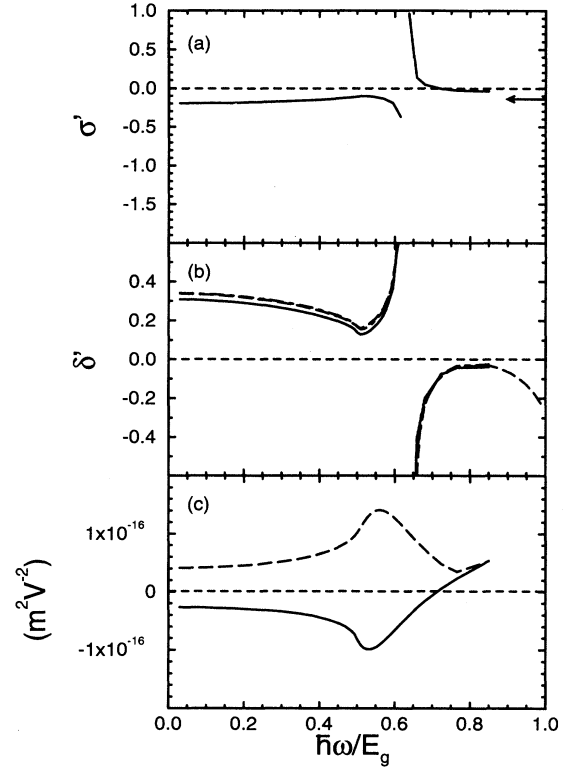
FIG. 3. Dispersion of the nonlinear refractive ratios for InSb: (a) shows the refractive anisotropy parameter with the arrow indicating the value of the ratio $-2E_g/(E_g + E_u)$ (see text); (b) shows the refractive incremental dichroism parameter, for the seven-band model (solid), the four-band model (dashed), and the incremental dichroism for $\mathbf{k} \parallel$ [111] (chain) (see text); (c) shows the products $\sigma'\chi'_{xxxx}$ (solid) and $\delta'\chi'_{xxxx}$ (dashed).

found to be the case for two-photon absorption.[11]

To illustrate more clearly the magnitude of the anisotropy, the orientation variation of n_2 [Eq. (14)] is shown plotted for both linear and circular polarized light in Fig. 4, for the case of GaAs at a frequency ω such that $\hbar\omega = E_g/2$, where $\sigma' = -0.82$ and $\delta' = 0.075$. For this example, n_2 is 55% larger for light polarized linearly along [111] compared to [100]; the anisotropy is illustrated clearly by the fact that the upper 3D plot in nowhere near to that of a sphere. Figure 5 shows the calculated dispersion of n_2 [Eq. (14)], including empirically the dispersion of the linear refractive index n_0.[36] The results are for the specific degenerate geometries under which there is no polarization rotation or induced ellipticity: linear polarization with $\hat{\mathbf{e}} \parallel$[100], [110], or [111] and circular polarization with $\hat{\mathbf{k}} \parallel$[100] or [111].

IV. DISCUSSION

The reported measurements that are the closest to providing a comparison with the present calculations are

those of Ref. 28. The quoted measurements are of the induced birefringence experienced by a noncollinear probe beam $\Delta n_2 = \left(\Delta n^\parallel - \Delta n^\perp\right)/I_e$, where $\Delta n^\parallel$ and $\Delta n^\perp$ are the refractive index changes induced by the excite beam for probe polarizations parallel and perpendicular to the excite polarization, respectively. The induced birefringence was measured for excite polarization parallel to [100] and [110], for propagation in the [001] direction. The results of Table II can be used to write the nonlinear index difference in terms of the three nonlinear refraction parameters,

$$\Delta n_2[100] = \frac{1}{I_e}\left(\Delta n^\parallel - \Delta n^\perp\right)_{\hat{e}\parallel[100]}$$
$$= n_2^L[001]\left(1 + \delta' + \tfrac{1}{2}\sigma'\right) , \qquad (24)$$
$$\Delta n_2[110] = \frac{1}{I_e}\left(\Delta n^\parallel - \Delta n^\perp\right)_{\hat{e}\parallel[110]}$$
$$= n_2^L[001]\left(1 + \delta' - \tfrac{1}{2}\sigma'\right) . \qquad (25)$$

Unfortunately a third measurement is necessary in order to determine all three parameters independently. Nevertheless, the ratio gives a simple combination of δ' and σ'
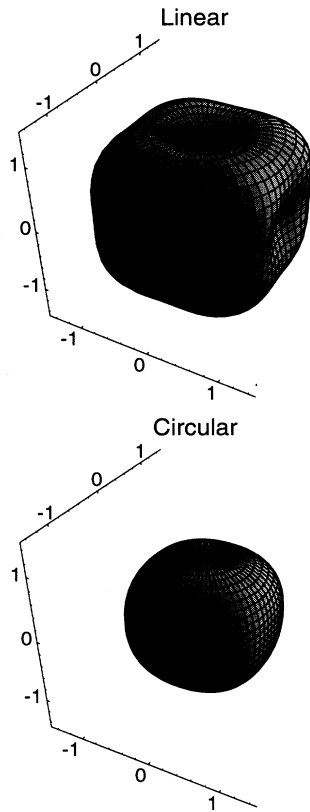
FIG. 4. The orientational dependence of the nonlinear refraction for GaAs at $\hbar\omega = E_g/2$ calculated from the present model, scaled to $n_2^L[001]$. For linear polarization, the variation is shown with respect to the polarization vector orientation (θ_p, ϕ_p) and for circular polarization, the variation is shown with respect to the propagation direction (θ, ϕ). In each case, the origin is at the center of the figure and magnitude of n_2 is proportional to the distance to the surface.
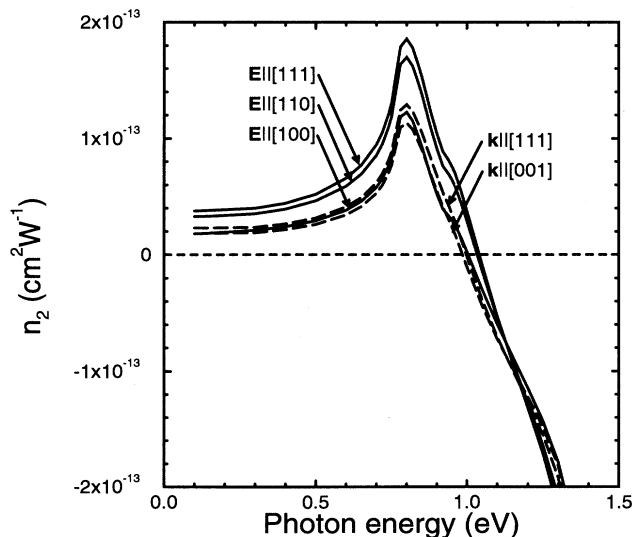

FIG. 5. The dispersion of the ultrafast nonlinear refraction coefficient n_2 for GaAs (low-temperature parameters) for the various polarization configurations indicated. The dispersion of the linear index is included empirically in determining this plot (Ref. 36).

and the difference gives the $\sigma' n_2^L[001]$ product.

The nonlinear refraction measurements on GaAs were made at 950 nm, where the photon energy is just below the band edge; $\hbar\omega/E_g = 0.92$ and the results were $\Delta n_2[100] = -3.3 \times 10^{-13}$ cm^2 W^{-1} and $\Delta n_2[110] = -5.0 \times 10^{-13}$ cm^2 W^{-1}. At the near-edge frequencies the two-photon resonant transitions contributing to Re$\chi^{(3)}$ occur for electronic wave vectors well removed from the Brillioun zone center, where the band-structure calculations are the most susceptible to approximations of the model. Nevertheless the observed ratio, $\Delta n_2[100]/\Delta n_2[110] = 0.66$, is close to the theoretical ratio of 0.73. If the value of δ' is accepted as being close to zero then the values of σ' and $n_2^L[001]$ inferred from the experiments are -0.4 and -4×10^{-13} cm^2 W^{-1} respectively. Again the result is close to the theoretical prediction of -3.5×10^{-13} cm^2 W^{-1}.

The measurements for CdTe at 950 nm also correspond to a frequency just beneath the one-photon band edge: $\Delta n_2[100] = -1.4 \times 10^{-13}$ cm^2 W^{-1} and $\Delta n_2[110] = -2.4 \times 10^{-13}$ cm^2 W^{-1}. Assuming a value for the dichroism parameter of $\delta' \simeq 0$ in this case also, implies the following values for the anisotropy and strength parameters: $\sigma' = -0.5$ and $n_2^L[001] = -1.9 \times 10^{-13}$ cm^2 W^{-1}.

The measurements on ZnSe at 950 nm, at a photon energy just below the half gap gave $\Delta n_2[100] = 0.14 \times 10^{-13}$ cm^2 W^{-1} and $\Delta n_2[110] = 0.34 \times 10^{-13}$ cm^2 W^{-1}. The results presented here for GaAs and InSb suggest it is reasonable to take the following range for possible values of the dichroism parameter for this frequency, $0 < \delta' < 1/3$. The experimental results then imply the following possible ranges for the strength and anisotropy parameters: 0.18×10^{-13} cm^2 W^{-1} $< n_2^L[001] < 0.24 \times 10^{-13}$ cm^2 W^{-1} and $-1.1 < \sigma' < -0.8$. The smaller magnitude of n_2 compared to GaAs is consistent with the larger fundamental band gap of ZnSe.

In Ref. 37, the ratio of cross-phase modulation on a TM probe ($\hat{p} \parallel [001]$) induced by a TE excite ($\hat{e} \parallel [110]$) to the self-phase modulation on the TE excite was measured for an Al$_{0.18}$Ga$_{0.82}$As wave guide at a photon energy corresponding to half the band gap. These effects were found to be approximately equal and the best fit gave a ratio of 0.95. Now this composition of Al$_x$Ga$_{1-x}$As has a band gap at room temperature similar to that for GaAs at low temperatures. At $\hbar\omega = E_g/2$ for GaAs, we calculate $\sigma' = -0.82$ and $\delta' = 0.075$, which predicts an identical ratio of cross-phase modulation to self-phase modulation of 0.95 for this geometry.

There are a variety of anisotropy parameters associated with third-order nonlinear effects for cubic materials. Here we have presented calculations for the anisotropy of nonlinear refraction, which corresponds to the real part of $\chi^{(3)}(-\omega,\omega,\omega)$. We have previously presented equivalent calculations for the anisotropy of two-photon absorption, which corresponds to the imaginary part of the same third-order susceptibility tensor element.[11] Additionally a similar form of anisotropy parameter can be obtained for third-harmonic generation, which corresponds to $\chi^{(3)}(\omega,\omega,\omega)$.[13,38] There is no simple relation between these three forms of anisotropy parameter; they have quite different dispersion relations. How-

ever, for GaAs, the parameters are of the same order of magnitude and in the long-wavelength limit the nonlinear refraction and third-harmonic generation coefficients are negative, as is the 2PA anisotropy in the range $E_g/2 < \hbar\omega < E_g$. In Ref. 17, the contribution to the scaling of the two-photon absorption anisotropy parameter from allowed-forbidden transitions due to the mixing of the higher-conduction-band set was estimated as approximately equal to $-2E_g/(E_g+E_u)$, where (E_g+E_u) is the valence to higher-conduction-band gap. This ratio takes the values of -0.68 for GaAs and -0.14 for InSb. For most of the frequency regime of the present calculations, the nonlinear refraction associated with two-photon resonant transitions dominates the strength of n_2. It is therefore not surprising that the same approximation gives a good measure for σ' as indicated by the arrows on Figs. 2(a) and 3(a). Using the simple formula to scale between materials, the anisotropy of GaAs is predicted to be around five times that of InSb. This has been verified in the case of two-photon absorption,[5] and proves here to be valid for the more detailed calculations over most of the transparency region.

It can be seen from Fig. 1 that Kleinmann symmetry is valid in the low frequency limit, i.e., $\chi'_{xxyy} = \chi'_{xyxy}$. In this limit the dichroism parameter can be written solely in terms of the anisotropy parameter, $\delta' = (1 + \sigma'/2)/3$. For an isotropic medium this takes the value of $1/3$.[8] The band-structure calculations for GaAs and InSb indicate that σ' is generally negative in the low frequency regime, and hence the dichroism parameter will have a smaller value than the isotropic results. This is a consequence of the use of $\chi^{(3)}_{xxxx}$ in the definitions of σ' and δ' in Eqs. (12) and (13). It may be noted that for propagation in

the [111] direction, for which the material behaves as if it were isotropic, the incremental dichroism does take the isotropic Kleinmann value of $1/3$ in the low frequency limit.

One of the applications of ultrafast nonlinear refraction is in the role of all-optical switching. In order to obtain switching, the required nonlinear phase shift must be achieved before losses reduce the irradiance. For the transparent spectral region beneath the one-photon band gap in semiconductors and for the high irradiances required for ultrafast nonlinear refraction, the dominant loss mechanism is usually two-photon absorption. In order to obtain all-optical switching, the figure of merit $|n_2|/\beta\lambda$ must exceed some critical value; this value depends on the device geometry but is always of the order of unity.[4] Over the spectral range $E_g/2 < \hbar\omega < E_g$ the all-optical switching condition is only satisfied for narrow ranges just above the half gap and just below the one-photon band edge.[1] The question to be addressed here is what effect does the anisotropy have on the all-optical switching figure of merit? In order to answer this, Fig. 6 shows the ratio $|\mathrm{Re}\chi^{(3)}_{\mathrm{eff}}|/\mathrm{Im}\chi^{(3)}_{\mathrm{eff}} = 4\pi|n_2|/\beta\lambda$ calculated for light linearly polarized parallel to the crystallographic directions [001] and [111] and for circularly polarized light propagating parallel to [001] (a similar plot is obtained for any circular polarization). In can be seen that although the figure of merit is modified by the anisotropy, it does not significantly alter the usable frequency range for all-optical switching.

V. CONCLUSIONS

In this paper the anisotropy of ultrafast nonlinear refraction in the zinc-blende semiconductors GaAs and InSb has been determined using the anisotropic band-structure model obtained with the inclusion of the Γ^c_{15} conduction-band set. It is found that the resulting orientational dependence of n_2 for frequencies below the two-photon band edge is substantial in GaAs but almost insignificant for InSb. This simply relates the different fundamental band gaps, which alters the relative mixing of the upper-conduction-band set with the lower-conduction band and valence bands. There is also predicted to be a significant dispersion in this anisotropy. The magnitude of the anisotropy is large in the long-wavelength limit; hence it is not too surprising that wide-gap cubic solids also seem to exhibit significantly anisotropic nonlinear refractive coefficients.[16,18-21] At frequencies above the two-photon band edge the dispersion of the anisotropy (and the dichroism) has a complex behavior. This is a manifestation of the change in sign of n_2, from positive at low frequencies to negative at high frequencies.

The anisotropy in the nonlinear refraction can manifest itself in two ways. First there is the obvious variation in magnitude for different crystalline orientations. Second, the anisotropy can produce an effective birefringence which, for appropriate polarization geometries, leads to a polarization state that changes upon propagation. For a purely refractive effect, a linearly polarized input can develop a degree of ellipticity. Such
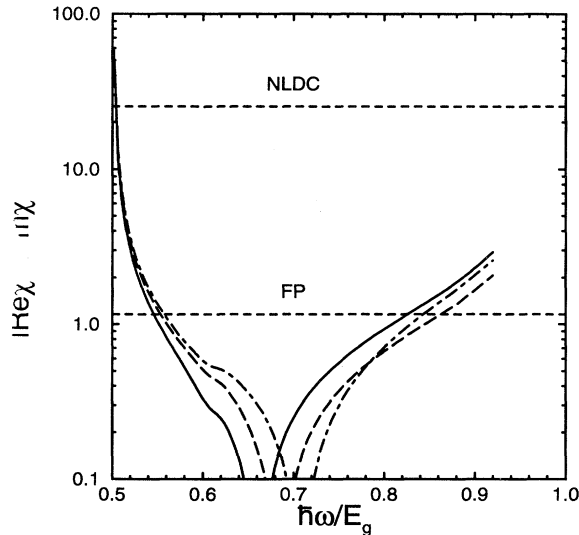
FIG. 6. Figure of merit for all-optical switching for low-temperature GaAs for light linearly polarized parallel to [001] (solid) and [111] (dashed) and for circularly polarized light propagating parallel to [001] (chain). Also shown are the limits that must be exceeded to obtain all-optical switching in a nonlinear directional coupler (NLDC) and a Fabry-Pérot interferometer.

a Kerr ellipticity has been used to measure the effect of anisotropy experimentally.[28] The present calculations are consistent with the few experimental measurements of anisotropy effects in zinc-blende semiconductors that have been made.

The formula $-2E_g/(E_g + E_u)$ proves to be useful first approximation for scaling the refractive index anisotropy parameter σ' between materials, as it was for the 2PA anisotropy parameter σ''.

[1] D. C. Hutchings and B. S. Wherrett, Phys. Rev. B **50**, 4622 (1994).

[2] J. S. Aitchison, A. H. Kean, C. N. Ironside, A. Villeneuve, and G. I. Stegeman, Electron. Lett. **27**, 1709 (1991).

[3] A. Villeneuve, C. C. Yang, G. I. Stegeman, C.-H. Lin, and H.-H. Lin, Appl. Phys. Lett. **62**, 2465 (1993).

[4] V. Mizrahi, K. W. DeLong, G. I. Stegeman, M. A. Saifi, and M. J. Andrejco, Opt. Lett. **14**, 1140 (1989).

[5] D. C. Hutchings and B. S. Wherrett, Phys. Rev. B **49**, 2418 (1994); J. Mod. Opt. **41**, 1141 (1994).

[6] M. Sheik-Bahae, D. C. Hutchings, D. J. Hagan, and E. W. Van Stryland, IEEE J. Quantum Electron. **27**, 1296 (1991).

[7] D. C. Hutchings, M. Sheik-Bahae, D. J. Hagan, and E. W. Van Stryland, Opt. Quantum Electron. **24**, 1 (1992).

[8] D. C. Hutchings and B. S. Wherrett, Opt. Commun. **111**, 507 (1994).

[9] E. W. Van Stryland, H. Vanherzeele, M. A. Woodall, M. J. Soileau, A. L. Smirl, S. Guha, and T. F. Boggess, Opt. Eng. **24**, 613 (1985).

[10] D. C. Hutchings and E. W. Van Stryland, J. Opt. Soc. Am. B **9**, 2065 (1992).

[11] D. C. Hutchings and B. S. Wherrett, Opt. Mater. **3**, 53 (1994).

[12] N. I. Zheludev and A. D. Petrenko, Kristallografiya **29**, 1045 (1983) [Sov. Phys. Crystallogr. **29**, 613 (1984)].

[13] G. Petrocelli, E. Pichini, F. Scudieri, and S. Martellucci, J. Opt. Soc. Am. B **10**, 918 (1993).

[14] S. J. Bepko, Phys. Rev. B **12**, 669 (1975).

[15] J. P. van der Ziel, Phys. Rev. B **16**, 2775 (1977).

[16] R. DeSalvo, M. Sheik-Bahae, A. A. Said, D. J. Hagan, and E. W. Van Stryland, Opt. Lett. **18**, 194 (1993).

[17] M. D. Dvorak, W. A. Schroeder, D. R. Andersen, A. L. Smirl, and B. S. Wherrett, IEEE J. Quantum Electron. **30**, 256 (1994).

[18] P. D. Maker and R. W. Terhune, Phys. Rev. **137**, A801 (1965).

[19] M. D. Levenson and N. Bloembergen, Phys. Rev. B **10**, 4447 (1974).

[20] R. Adair, L. L. Chase, and S. A. Payne, Phys. Rev. B **39**, 3337 (1989).

[21] M. D. Johnson and K. R. Subbaswamy, Phys. Rev. B **39**, 10 275 (1989).

[22] A. A. Borshch, M. S. Brodin, and V. N. Semioshko, Phys. Status Solidi A **91**, 135 (1984).

[23] T. F. Boggess, A. L. Smirl, and B. S. Wherrett, Opt. Commun. **43**, 128 (1982).

[24] M. J. Snelling, P. Perozzo, D. C. Hutchings, I. Galbraith, and A. Miller, Phys. Rev. B **49**, 17160 (1994).

[25] A. I. Kovrighin, D. V. Yakovlev, B. V. Zhdanov, and N. I. Zheludev, Opt. Commun. **35**, 92 (1980).

[26] M. G. Dubenskaya, R. S. Zadoyan, and N. I. Zheludev, J. Opt. Soc. Am. B **2**, 1174 (1985).

[27] S. A. Akhmanov, N. I. Zheludev, and R. S. Zadoyan, Zh. Eksp. Teor. Fiz. **91**, 984 (1986) [Sov. Phys. JETP **64**, 579 (1986)].

[28] W. A. Schroeder, D. S. McCallum, D. R. Harken, M. D. Dvorak, D. R. Andersen, and A. L. Smirl, J. Opt. Soc. Am. B **12**, 401 (1995).

[29] N. Pfeffer, F. Charra, and J. M. Nunzi, Opt. Lett. **16**, 1987 (1991).

[30] P. N. Butcher and D. Cotter, *The Elements of Nonlinear Optics*, edited by P. L. Knight and W. J. Firth, Cambridge Studies in Modern Optics Vol. 9 (Cambridge University Press, Cambridge, England, 1990).

[31] D. C. Hutchings, J. S. Aitchison, B. S. Wherrett, G. T. Kennedy, and W. Sibbett, Opt. Lett. **20**, 991 (1995).

[32] E. O. Kane, J. Phys. Chem. Solids **1**, 249 (1957).

[33] P. Pfeffer and W. Zawadzki, Phys. Rev. B **41**, 1561 (1990).

[34] B. S. Wherrett, Proc. R. Soc. London, Ser. A **390**, 3736 (1983).

[35] W. Zawadzki, I. T. Yoon, C. L. Littler, X. N. Song, and P. Pfeffer, Phys. Rev. B **46**, 9469 (1992).

[36] S. Adachi, J. Appl. Phys. **58**, R1 (1985).

[37] A. Villeneuve, J. U. Kang, J. S. Aitchison, and G. I. Stegeman, Appl. Phys. Lett. (to be published).

[38] D. J. Moss, E. Ghahramani, J. E. Sipe, and H. M. van Driel, Phys. Rev. B **41**, 1542 (1990).